

PowerEnergy2016-59416

MULTIFUNCTIONAL ENERGY STORAGE COMPOSITES - DESIGN, FABRICATION, AND EXPERIMENTAL CHARACTERIZATION

Purim Ladpli
Stanford University
Stanford, CA, USA

Raphael Nardari
Stanford University
Stanford, CA, USA

Raunaq Rewari
Stanford University
Stanford, CA, USA

Hongjian Liu
Farasis Energy Inc.
Hayward, CA, USA

Michael Slater
Farasis Energy Inc.
Hayward, CA, USA

Keith Kepler
Farasis Energy Inc.
Hayward, CA, USA

Yinan Wang
Stanford University
Stanford, CA, USA

Fotis Kopsaftopoulos
Stanford University
Stanford, CA, USA

Fu-Kuo Chang
Stanford University
Stanford, CA, USA

ABSTRACT

We propose the concept of Multifunctional-Energy-Storage Composites (MES Composites) which highlights a unique integration technique for embedding lithium-ion battery materials in structural carbon-fiber-reinforced-polymers (CFRP). Unlike standard lithium-ion pouch cells, the MES Composites maximizes material utilization by using CFRP facesheets to house the electrochemistry. Through-thickness polymer reinforcements are implemented to allow load transfer between the two facesheets, analogous to the sandwich structure construction.

In this work, the design rationale, materials and fabrication techniques, experimental evaluation, and performance of the first-generation MES Composites will be presented. MES Composite cells with a nominal capacity of approximately 4 Ah, with various reinforcements-array configurations, were fabricated and first tested through a series of electrochemical reference performance tests (RPT) under a strain-free condition. The MES Composite cells then underwent a mechanical-electrical-coupling test, where a quasi-static three-point-bending load was applied at increasing increments. Mechanical testing was interrupted after each increment to perform a sequential RPT to quantify any non-catastrophic degradation in the electrochemical performance.

The obtained results verify the feasibility of the concept showing that the electrochemical performance of the MES Composites can be maintained at the same level as the regular lithium-ion battery. The reinforcement architecture of the MES

Composite constrains the relative motion of the battery electrodes and increases the bending rigidity, resulting in a higher load carrying capacity and inhibiting non-fatal injury of the cell under mechanical loads. This multifunctional material system can also be scaled up and ultimately provide considerable weight and volume saving at the system level.

INTRODUCTION

Owing to the substantial benefits from reducing fossil fuel consumption and decreasing emissions, the past few decades has seen accelerating introduction electric vehicles (EVs). However, there is still a considerable challenge in improving the efficiency and decreasing the cost of these systems, resulting in the slow worldwide adoption of EVs [1]. A multifunctional, safety-centric approach, where the energy storage is also designed to simultaneously and synergistically carry mechanical loads and assist vehicle crash management, has thus been introduced [1, 2, 3]. A multifunctional design removes the redundancy between the unifunctional subcomponents, resulting in improvements in system-level performance, weight reduction, and cost savings.

Intensive research effort is underway to develop multifunctional energy-storage structures. Literature survey reveals one research discipline which focuses on formulating the constituent materials to be intrinsically capable of storing energy as well as carry mechanical loads. For instance, Liu [4] used electrolyte-filled polymer matrix as a binder to laminate conventional lithium-ion (Li-ion) battery electrode layers. In other work, Greenhalgh [5] and Snyder [6] fabricated CFRP

supercapacitors, by combining the intrinsic electrochemical nature of carbon fibers and polymer-based electrolyte matrix. However, the energy density of these structural energy-storage materials was still considerably low, as material modifications to achieve better mechanical performance significantly impaired the electrochemistry. Otherwise, a great amount of energy density has to be sacrificed to achieve useful mechanical performance.

Another strategy aims at modifying and optimizing the existing structural materials to serve as a secondary, mechanical enclosure for pre-packaged commercial batteries. For example, parts of the core material in sandwich panels were displaced and substituted with commercial off-the-shelf Li-ion pouch cells [7-8]. However, these systems still lacked the synergy between the disparate, unifunctional subcomponents. Disbonds and limited load transfer between the cells and the structural enclosure prevented the inherent structural properties of the battery to be harnessed.

This paper presents the development of the Multifunctional Energy Storage Composites (MES Composites). The MES Composites features a unique integration method - an intermediate strategy - that allows the functional secondary-battery materials, including but not limited to Li-ion battery materials, to be directly embedded in structural CFRP. The concept leverages the feasibility of using CFRP as the electrochemistry housing and the inherent mechanical properties of the battery materials, and achieve multifunctionality by permitting the two parts to be mutually beneficial.

METHOD OF APPROACH

State-of-the-art automotive Li-ion pouch cells contain a stack of thin anode and cathode layers, arranged in an alternating fashion. Each adjacent electrode pair is separated by a thin polymer separator membrane (Figure 1 (a)). The stack is packaged in a thin aluminum-polymer-laminate pouch, filled with organic liquid electrolyte, and vacuum-sealed. The individual layers are loose, i.e. mechanical linkage is not present between the layers. Thus load transfer through the cells is minimal if any. Conventional Li-ion pouch batteries are not designed to carry mechanical loads, which might cause excessive relative sliding between the layers and short-circuit the cell.

MES Composite Architecture. The proposed concept of Multifunctional-Energy-Storage Composites (MES Composites) encapsulates lithium-ion battery materials inside structural carbon-fiber-reinforced-polymers (CFRP) ‘facesheets’ (Figure 1 (b)). The energy-storage component of the MES Composites is standard automotive Li-ion battery active materials. Instead of using the standard aluminum-laminate packaging, the MES Composites also uses the CFRP facesheets to contain the electrodes and the liquid electrolyte.

Similar to a sandwich structure construction, the stiff, structural CFRP facesheets are placed on either side of the electrode stack, separated by the stack thickness, to carry the bending moment. This increases the moment of inertia of the laminate, resulting in a higher bending rigidity [9]. However,

without the interlayer shear resistance of the battery core, the thin battery layers will bend about their own individual neutral axis, and the structural contribution from the facesheets will be minimal.

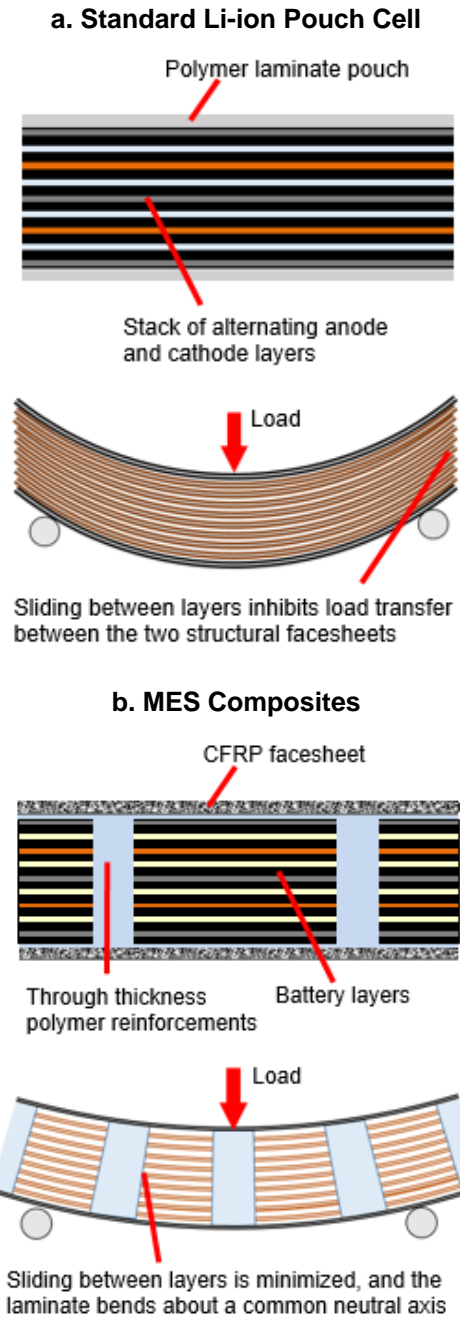


Figure 1. Comparison between (a. Top) standard Li-ion pouch cells and (b. Bottom) MES Composites. MES Composites employ through-thickness reinforcements which transfer mechanical loads between two structural facesheets and improve shear resistance of the battery core

In the MES Composites, we use through-thickness polymer reinforcement pillars, which extend through the perforations in the electrode stack and mechanically link the two structural CFRP facesheets on either side together, similar to the Lithylene technology [10]. The through-thickness reinforcements enable load transfer between the two facesheets and inhibit the relative slipping between the adjacent electrode layers. This significantly increases the stiffness and strength of the MES Composites over regular lithium-ion batteries as the entire laminate is able to bend about a common neutral axis.

The MES Composites are capable of simultaneously providing a high mechanical load-carrying capability, as well as storing electrical energy. By permitting the two materials to be mutually beneficial and become multifunctional, weight and volume of the MES-Composites-powered devices can be minimized.

SAMPLES AND FABRICATION

Four types of samples were fabricated and tested electrochemically and mechanically in this work, as summarized in Table 1.

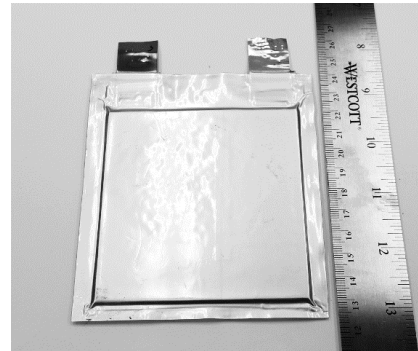
Table 1. Sample Types and Description

Sample Type	Sample Description	Electrochemical Characterization	Mechanical Testing	Dimensions & Weight
A	Al-laminate packaging No perforations	✓		90x90x3.5 mm 81±1 g
B	MES Composite No perforations		✓	160x110x5 mm (110x110x5 mm – functional) 120±5 g
C	MES Composite 4x4 perforation array	✓	✓	160x110x5 mm (110x110x5 mm – functional) 120±5 g
D	MES Composite 5x5 perforation array	✓	✓	160x110x5 mm (110x110x5 mm – functional) 120±5 g

Sample A (Figure 2 (Top)) was essentially a standard 4.6Ah Li-ion pouch cell, encapsulated in a conventional aluminum-laminate packaging. Its purpose was to serve as a baseline for electrochemical characterization. Mechanical testing was not performed on this sample type, as discussed in the subsequent section.

Samples B, C, and D (Figure 2 (Bottom)) were MES Composites, with Li-ion battery active materials encapsulated in CFRP facesheets. All of them except Sample B underwent both electrochemical characterization and mechanical testing. The difference between Samples B, C and D was the density of the through-thickness reinforcement array. Sample B did not have any through-thickness reinforcements, while Samples C and D contained 4x4 and 5x5 arrays of equally-spaced cylindrical reinforcements respectively (Figure 3). The active electrode stack for all sample types consisted of 11 and 10 90x90mm double-sided anode and cathode layers respectively.

Sample A



Samples B, C, D (Exterior)



Figure 2. Manufactured samples (Top) Sample A – Non-perforated electrode stack packaged in aluminum-laminate pouch (Bottom) MES Composite Samples B, C, D with the same external dimensions

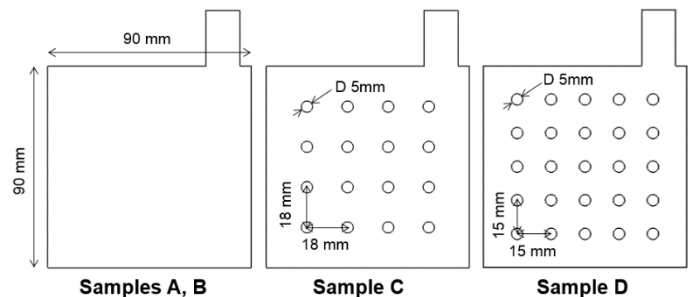


Figure 3. Anode dimensions and locations of perforations for Samples A and B (Left), Sample C (Middle), and Sample D (Right)

An MES Composite cell comprises the following three main components: the core battery electrode stack, the CFRP facesheets, and the polymer reinforcements.

Electrode Stack. The battery core is constructed from a stack of alternating anode and cathode layers, with each adjacent layer separated by a thin microporous polymer separator. Conventional production active materials were used for the cathode and the anode, which were Lithium Nickel-Cobalt-Manganese (NCM) and graphite respectively. All the sample types used 11 anode and 10 cathode layers – the external electrode dimensions measured 90mm x 90mm.

The electrodes were cut and perforated at the locations where the through-thickness reinforcements will be placed, prior to lamination. The patterns of the through-thickness reinforcement array for the different sample types are shown in Figure 3, for anode. A separate design for the cathode was made such that the anode coverage is slightly larger than the cathode (0.5 mm in every direction) to ensure that excess anode was present and reduce the possibility of shorting. After stacking, the separators were spot-melted to bridge the through-thickness holes. The cathode's copper current collectors were ultrasonically welded together onto a nickel tab, and similarly for the anode's aluminum current collectors using an aluminum tab.

The thickness of the complete electrode stack measured approximately 3.5 mm. For Sample A, the stack was then pouched in a standard aluminum-laminate packaging. For Samples B, C, and D, the electrode was subsequently encapsulated in the CFRP facesheets, as will be described.

CFRP Facesheet. Dry 3K 2x2-Twill T300 carbon fiber fabric (Toray) was used in a vacuum-assisted resin infusion process to fabricate the CFRP facesheets. Three carbon fiber layers ([0,90] orientation) were infused with the unmodified liquid epoxy system (Bisphenol A diglycidyl ether (DGEBA) + Triethylene tetramine (TETA) (stoichiometric), Sigma Aldrich). The laminate was then cured at room temperature for 24 hours, followed by a post-cure at 90°C for 30 minutes. The laminate was then cut into 110mm x 160mm facesheet pieces.

Polymer Reinforcements and Assembly. An edge-filling polymer frame is cut from a 3.5mm-thick sheet of thermoplastic, into the dimensions as shown in Figure 4 (Left). The frame serves to contain the electrolyte within the electrode stack core. The frame width of 10 mm in this case is more than sufficient for electrolyte containment. The length of the frame (and CFRP facesheets) was designed to be 160 mm to allow for 30 mm overhangs in a three-point-bending test, as will be discussed further.

The perforations in the electrode stack were then filled with thermoplastic polymer plugs, placed inside the opening of the edge-filling polymer frame, and sandwiched between two facesheets (Figure 4 (Right)). The assembly was hot-pressed to melt and fuse the polymer reinforcements to the facesheets. The cell was filled with a standard Li-salt electrolyte (LiPF₆ in EC/DMC/DEC organic solvent), edge-sealed, formed, degassed,

and re-sealed. It should be noted that even without the standard Li-ion battery pouch, the cell could subsequently undergo a standard cell fabrication process, as the facesheets and the polymer frame serve as the cell enclosure.

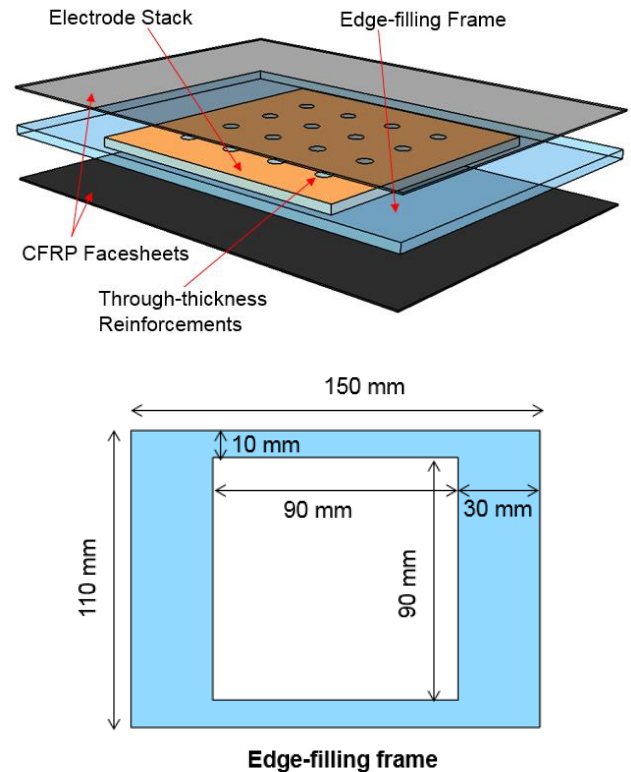


Figure 4. (Top) MES Composite assembly and internal components; (Bottom) Dimensions of the edge-filling frame

EXPERIMENTAL CHARACTERIZATION

Electrochemical Characterization. The MES Composites require a thorough electrochemical feasibility characterization, namely the apparent cell capacity, cell impedance, and most importantly the cycle life performance, as its construction significantly differs from that of a conventional Li-ion cell.

After a solid electrolyte interphase (SEI) formation step, the Samples A, C and D were first subject to an initial slow-rate charge-discharge cycle between 3.0V – 4.2V, where the testing protocol was calibrated to obtain the C-rate (1C-rate is the rate at which the battery will be fully charged or discharged in 1 hour).

The samples then underwent the initial electrochemical Reference Performance Test (RPT). The cells were cycled at a C/3 (3 hours to fully charge or discharge the cell) rate, or approximately at 1300 mA. At the beginning of life (BOL) of each sample, the cell DC impedance was also measured. The test

was performed using a Hybrid Pulse Power Characterization (HPPC) test profile during the first C/3 discharge. The technique evaluates the cell DC impedance at every 10% of Depth of Discharge (DoD) by measuring the voltage difference during the current interruption.

The C/3 charge-discharge cycle was repeated to compare the retention of discharge capacity with increasing number of cycles between the different samples types.

Mechanical Testing. A flexural (three-point bending) test was performed on Samples B, C, and D after the initial electrochemical RPT, to evaluate the mechanical feasibility of the MES Composites. The interlayer-shear inhibition capability of the through-thickness reinforcements could be validated through measuring and comparing the sample's bending rigidity.

Testing was performed on a three-point bending fixture with cylindrical-roller load applicator and supports using a 100mm span, on an MTS test system (Figure 5). The span allowed for an overhang of 30 mm on either side of the samples (lengthwise direction). The support span was approximately 20 times the depth, which was sufficient to avoid significant influence from transverse shear. The displacement at the mid-span was constantly measured while the crosshead was displaced at the rate of 0.127 mm/mm/min (quasi-static). The bending rigidity can be determined from the slope of the load-displacement curve using Equation 1.

$$EI = \frac{L^3}{48} \frac{dP}{d\delta_p} \quad (1)$$

Where EI is the effective bending rigidity, L is the support span, and $dP/d\delta_p$ is the slope of the load-displacement curve, in which P is the load and δ_p is the resulting mid-span displacement.

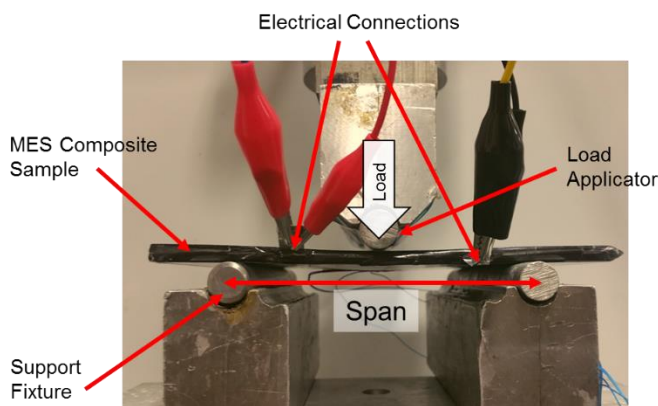


Figure 5. Three-point-bending test setup for Samples B, C, and D

The mechanical testing was interrupted when the mid-span deflection reached 1mm. After that, the sample was removed from the mechanical test machine, and a sequential electrochemical RPT was performed. The test was then repeated for a mid-span deflection of 2 mm.

The discharge curves, discharge capacity, and DC impedance before loading (pristine sample condition) could be compared with the results after mechanical load has been applied. This serves to indicate any non-fatal degradation in the battery performance due to mechanical loading.

RESULTS AND DISCUSSION

Electrochemical Characterization. Figure 6 presents the voltage and current history with time of a nominal C/3 cycle of a typical MES Composite Sample C, showing the typical inherent characteristics of the graphite/NMC chemistry. The charge-discharge current was 1300 mA (approximately C/3).

The apparent first discharge capacity was summarized in Table 2, for the MES Composite cells (Samples C and D) and the control Sample A, in comparison with the theoretical values. The theoretical capacity of each cell type can be calculated from the active material loading and the remaining surface area after perforation.

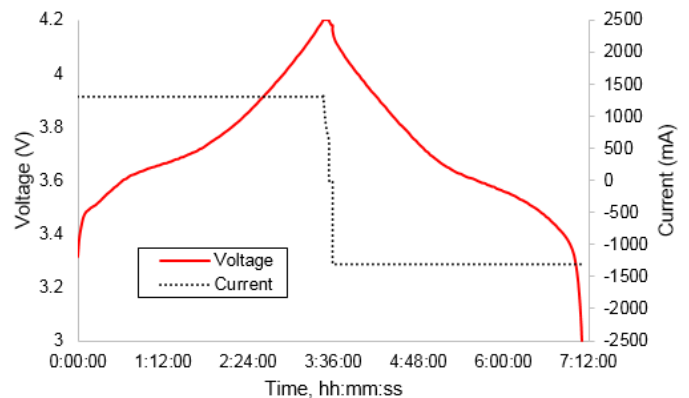


Figure 6. Voltage and current time-history for a nominal cycle of Sample C at C/3 rate

Table 2. Summary of first discharge capacity, in comparison with the theoretical capacity calculated from the added amount of active materials

Sample Type	Sample Description	Active Surface Area per Layer	Theoretical Capacity	Measured First Discharge Capacity
A	Al-laminate packaging No perforations	7921 mm ² (100%)	4602 mAh (100%)	4602 mAh (100%)
C	MES Composite 4x4 perforation array	7469 mm ² (94.3%)	4340 mAh (94.3%)	4243 mAh (92.2%)
D	MES Composite 5x5 perforation array	7215 mm ² (91.1%)	4192 mAh (91.1%)	3974 mAh (86.4%)

As expected, the apparent first discharge capacity of the MES Composite cells decreased as the loss of area increased due to the perforations in Samples C and D respectively. The active surface area in Sample C was 94.3% of that in Sample A due to the 4-by-4 perforations, and 91.1% for the case of Sample D.

Yet, it can be observed that the measured first discharge capacity of the MES cells were marginally lower than the predicted values (2.1% for Sample C and 4.7% for Sample D), but still within an acceptable extent. The discrepancies were thought to be linked partly to the slightly higher DC impedance in the MES Composites, shown in Figure 7. At 50% DoD, the DC impedance of Sample A (baseline) was 23 mΩ, whereas the impedance was measured to be approximately 31 mΩ for Samples C and D, approximately 35% higher.

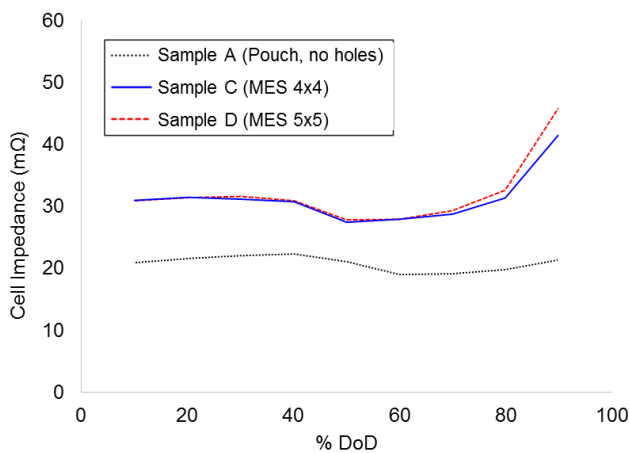


Figure 7. Cell DC impedance calculated from the HPPC test profile during a C/3 discharge (1 hour rest, 30s 1C discharge pulses)

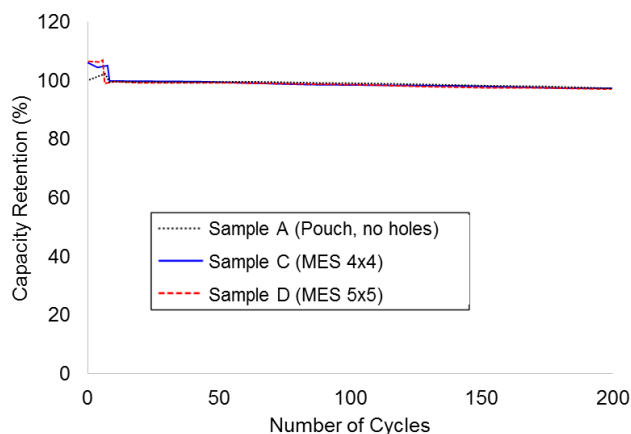


Figure 8. Capacity retention, in percentage of the first discharge capacity, with increasing cycle number for Samples A, C and D

The capacity hit and high impedance were likely due to the perforations and the non-standard cell build. The perforated electrodes in MES Composite Samples C and D have more free edges (holes edges) than the non-perforated Sample A. Imperfections from electrode cutting, such as edge burrs and active material flaking, would be more pronounced for the perforated electrodes. Also, with more free edges than a regular cell, slight misalignment between adjacent anode-cathode pairs can cause a greater loss in the actual active surface area, resulting in a reduction in cell capacity. The high-temperature, high-pressure assembly process might also cause the electrode layers and separator to deform or wrinkle, and impair the ionic pathway. Lastly, there might also be a negative impact on the electrochemistry and thus the cell capacity from the presence of the facesheet and polymer reinforcement materials.

Figure 8 shows the C/3-cycle capacity retention with increasing cycle number of the MES Composites Samples C and D, in comparison with the baseline Sample A. The capacity retention of the MES Composites, with respect to the initial discharge capacity, was found to be approximately 96% after 200 cycles, similar to the cycle-life performance of the baseline cell. The capacity fade of MES Composites is on par with commercial-grade production Li-ion batteries, despite of substantial deviation in the architecture and fabrication from conventional Li-ion pouch cells.

In summary, the electrochemical characterization has shown that a working MES Composite can be successfully fabricated and has electrochemical capability that is comparable to conventional Li-ion batteries. Slight modifications will be made in the upcoming iterations to optimize their performance, particularly on the apparent cell capacity and impedance.

Mechanical Testing. The typical load versus mid-span displacement curves for the three point bending of Samples B, C, and D are shown in Figure 9. The curves were found to be linear up to the maximum deflection (2 mm) applied during this experiment, and the slope values were repeatable for the different load-unload instances. The slope values were calculated through linear regression on the load-displacement data in the 0 – 0.5 mm deflection region. The ‘effective’ bending rigidity was then found using Equation 1, and summarized in Table 3.

It can be seen that the effective stiffness of Sample C (4x4 MES cell) was 11.0 Nm², which was as high as 4.4 times that of Sample B (non-perforated MES cell) at 2.5 Nm². The significant increase in rigidity can be attributed to the presence of the through-thickness reinforcements that effectively prevent the sliding motion between the layers and allow load transfer between the two facesheets. The bending rigidity ratio increased to 4.8 for Sample D, as the reinforcement array density increased to 5-by-5. Intuitively, the denser the reinforcement array, the greater the bending rigidity becomes. However, this comes with trade-off in the reduction of active material volume, and consequently lower energy density. This clearly poses an optimization problem to the design of the next generation MES Composites.

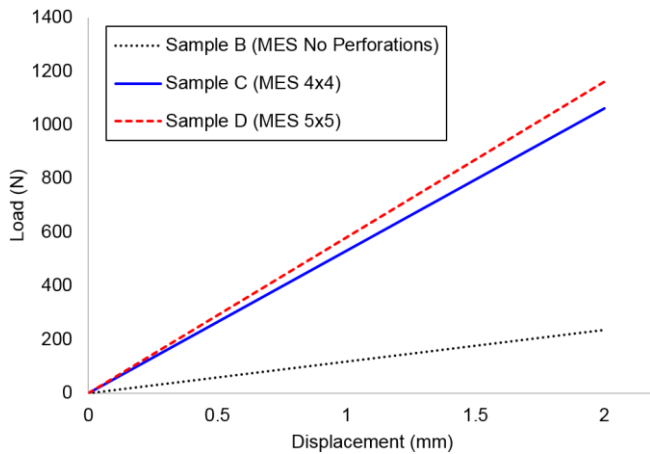


Figure 9. Load-displacement curves from the three-point bending test for representative Samples B, C, and D

Table 3. Summary of load-displacement slopes (load per unit mid-span displacement) and calculated effective bending rigidity

Sample Type	Sample Description	Load-displacement Slope	Effective Bending Rigidity
B	MES Composites No perforations	118 ± 10 N/mm	2.5 ± 0.3 Nm ²
C	MES Composite 4x4 perforation array	530 ± 7 N/mm	11.0 ± 2.0 Nm ²
D	MES Composite 5x5 perforation array	580 ± 20 N/mm	12.1 ± 0.7 Nm ²

Figure 10 shows the C/3 discharge voltage time-history of Sample D before loading (pristine), and after mid-span bending deflection of 1 mm (corresponding load of 530 N), and 2 mm (1160 N) respectively. Similarly to Sample B and C, there is only a slight deviation in the discharge time history with increase in mechanical load levels.

The normalized C/3 discharge capacity and cell impedance (at 50% DoD) after exposure to the incremental quasi-static loads are shown in Figure 11 and Figure 12 respectively. The results after load application were normalized, in percentage, with the values at pristine condition (100% - leftmost column of each cluster). This concurs with the results in the discharge curves - that is, no clear trend could be seen in the capacity and cell impedance results with increasing loading.

Up to the maximum mid-span deflection (2 mm over 100 mm span) in this test, no observable degradation due to the quasi-static load could be seen in the MES Composites. Moreover, it is worth noting that, at the same level of deflection (2 mm over 100 mm span), the load carrying capability has increased from 235N to 1060N, and 1160N, for the non-perforated, 4x4, and 5x5 MES cells respectively. This illustrates that the CFRP encapsulation and through-thickness reinforcement are capable of maintaining the integrity of the battery and the electrical connection and

preventing non-fatal electrochemical injury that could have come from mechanical loads.

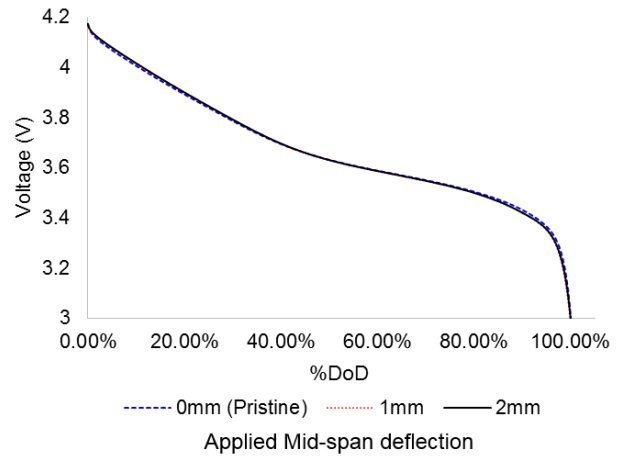


Figure 10. Voltage versus depth of discharge (DoD) for a C/3 discharge of a representative Sample D at the pristine condition, and after 1mm and 2mm mid-span mechanical bending has been applied.

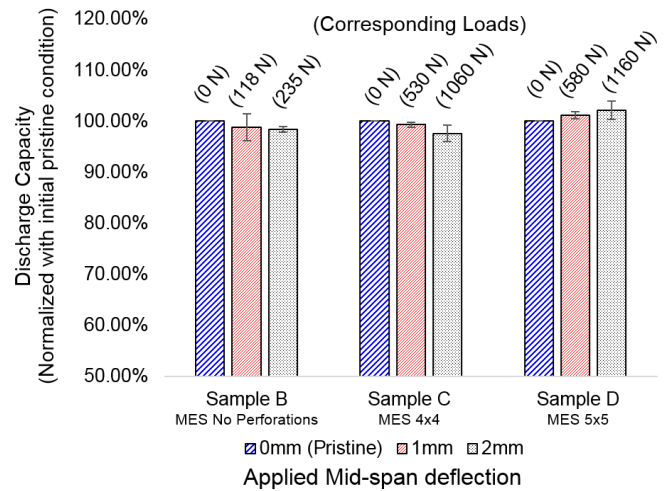


Figure 11. Effects on discharge capacity due to mechanical bending loads for Samples B, C, and D. Normalized discharge capacity after 1 and 2 mm deflection has been applied at mid-span, in comparison with that at pristine condition.

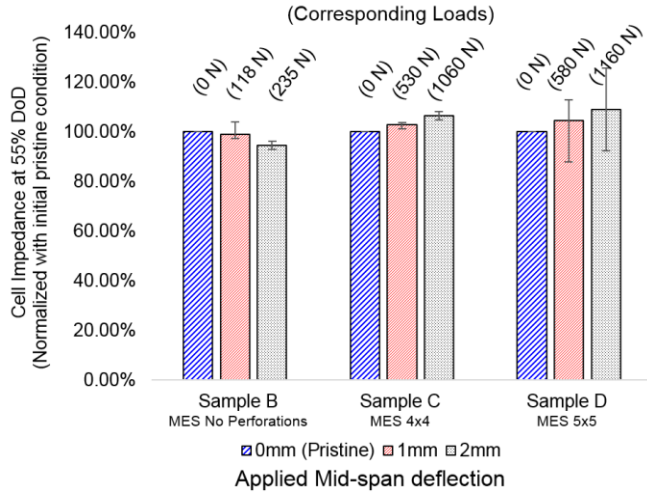


Figure 12. Effects on cell DC impedance due to mechanical bending loads for Samples B, C, and D. Normalized cell impedance at 50% DoD after 1 and 2 mm deflection has been applied at mid-span, in comparison with that at pristine condition.

Summary of Figures of Merits. The summary of the figures of merit of the different sample types is shown in Table 4. The C/3 discharge capacity for Sample A is 4.602 Ah. At a nominal cell voltage of 3.7 V, the cell energy thus becomes 17.0 Wh. Sample A weighs 81 g, and has the total volume of 28.4 mL, resulting in the gravimetric and volumetric energy density of 210 Wh/kg and 599 Wh/L respectively. Similar calculations can be carried out for Samples B, C, and D, and summarized in Table 4.

It can be seen that by adopting the MES Composite concept to li-ion battery materials, we were able to obtain a cell with bending rigidity close to as much as 20 times higher than that of a regular pouch cell. This comes with approximately 40% and 60% sacrifice in the gravimetric and volumetric energy density. Even though, the energy storage performance might be sub-optimal if considered individually, structural components at the system level can be replaced with the multifunctional MES Composites, potentially resulting in the system-level weight and space savings.

Table 4. Summary of Figures of Merits

Sample Type	Sample Description	Bending Rigidity	Gravimetric Energy Density	Volumetric Energy Density
A	Al-laminate packaging No perforations	(0.6 Nm ^{2*})	210 Wh/kg	599 Wh/L
B	MES Composite No perforations	2.5 Nm ²	142 Wh/kg	281 Wh/L
C	MES Composite 4x4 perforation array	11.0 Nm ²	131 Wh/kg	259 Wh/L
D	MES Composite 5x5 perforation array	12.1 Nm ²	123 Wh/kg	243 Wh/L

* Estimated from the published values [11], and adjusted for the difference in the cross-section geometry and moment of inertia

CONCLUSION

In this work, we have presented the design, fabrication process, and results from the characterization of the first generation Multifunctional Energy Storage (MES) Composites. It has been shown that the MES Composites can concurrently carry mechanical loads and store energy. The MES Composites utilizes through-thickness polymer reinforcement pillars that penetrate through perforations in the Li-ion battery electrode stack. The through-thickness reinforcements provide substantial mechanical integrity to the cell by rigidly linking the structural CFRP facesheets on either side, which also serves as a containment for the electrolyte. The preliminary results have illustrated that:

- Despite being vastly different from a standard Li-ion pouch cell, the MES Composites shows electrochemical performance, which is on par with traditional batteries.
- The through-thickness reinforcements significantly increases the bending rigidity by effectively preventing relative shearing of the electrode layers, allowing the structural facesheets to be efficiently utilized.
- The architecture of the MES Composites also helps keep the active electrochemical materials inside the cell intact under mechanical loads. At the maximum bending deformation (2 mm over 10 cm span) tested in this work, the best performing MES Composite can carry up to 1160N of bending load without observable degradation on electrochemical performance.

Further work is ongoing in the areas of manufacturing improvements, design optimization, and investigation on effects from various loading scenarios. Yet, it has been shown that the MES Composites can simultaneously function as both an energy storage as well as a load-carry member. The MES Composites can serve as a building-block material that can be scaled up to build structural components, with built-in energy-storage capability, for various application, and potentially resulting in a light-weight multifunctional system.

ACKNOWLEDGEMENTS

The authors gratefully acknowledge the support from the Advanced Research Projects Agency - Energy (U.S. Department of Energy) through the ARPA-E Award No. DE-AR0000393.

REFERENCES

- [1] Lynch, J., & Loh, K. (2006). A Summary Review of Wireless Sensors and Sensor Networks for Structural Health Monitoring. *The Shock and Vibration Digest*, 38(2), 91-128.
- [2] Salowitz, N., Guo, Z., Li, Y.-H., Kim, K., Lanzara, G., & Chang, F.-K. (2012). Bio-inspired stretchable network-based intelligent composites. *Journal of Composite Materials*, 47(1), 97-105.

- [3] Salowitz, N., Guo, Z., Roy, S., Nardari, R., Li, Y.-H., Kim, S.-J., Kopsaftopoulos, F., Chang, F.-K. (2013). A vision on stretchable bio-inspired networks for intelligent structures. 9th International Workshop on Structural Health Monitoring, (pp. 35-44). Stanford.
- [4] Liu, P., Sherman, E., & Jacobsen, A. (2009). Design and fabrication of multifunctional structural batteries. *Journal of Power Sources*, 189(1), 646-650.
- [5] Shirshova, N., Qian, H., Shaffer, M., Steinke, J., Greenhalgh, E., Curtis, P., Kucernak A., Bismarck, A. (2013). Structural composite supercapacitors. *Composites Part A: Applied Science and Manufacturing*, 46, 96-107.
- [6] Snyder, J., O'Brien, D., Baechle, D., Mattson, D., & Wetzel, E. (2008). Structural Composite Capacitors, Supercapacitors, and Batteries for U.S. Army Applications. ASME 2008 Conference on Smart Materials, Adaptive Structures and Intelligent Systems, 1, pp. 1-8. Ellicott City, Maryland, USA.
- [7] Thomas, J., Qidwai, S., Pogue III, W., & Pham, G. (2012). Multifunctional structure-battery composites for marine systems. *Journal of Composite Materials*, 47(1), 5-26.
- [8] Roberts, S., & Aglietti, G. (2008). Satellite multi-functional power structure: Feasibility and mass savings. *Journal of Aerospace Engineering*, 222(1), 41-51.
- [9] Allen, H. (1969). *Analysis and Design of Structural Sandwich Panels*. Oxford: Pergamon Press.
- [10] Notten, P., Ouwerkerk, M., van Hal, H., Beelen, D., Keur, W., Zhou, J., & Feil, H. (2004). High energy density strategies: from hydride-forming materials research to battery integration. *Journal of Power Sources*, 129(1), 45-54.
- [11] Sahraei, E., Hill, R., & Wierzbicki, T., (2012). Calibration and finite element simulation of pouch lithium-ion batteries for mechanical integrity. *Journal of Power Sources*, 201(2012), 307-321.